75N 10006

NASA TECHNICAL NOTE

NASA TN D-7749

NATIONAL AERONAUTICS AND SPACE ADMINISTRATION U.S.A.

NASA TN D-7749

EXTRACTION FROM FLIGHT DATA OF LATERAL AERODYNAMIC COEFFICIENTS FOR F-8 AIRCRAFT WITH SUPERCRITICAL WING

by James L. Williams and William T. Suit

Langley Research Center

Hampton, Va. 23665

AMERICAN REVOLUTION BICENTENNIAL 1776-1976

NATIONAL AERONAUTICS AND SPACE ADMINISTRATION • WASHINGTON, D. C. • NOVEMBER 1974

1. Report No. NASA TN D-7749	2. Government Accession No.	3. Recipient's Catalog No.
4. Title and Subtitle EXTRACTION FROM FLIGHT DATA OF LATERAL AERODYNAMIC COEFFICIENTS FOR F-8 AIRCRAFT WITH SUPERCRITICAL WING		5. Report Date November 1974
		6. Performing Organization Code
7. Author(s) James L. Williams and William T. Suit		8. Performing Organization Report No. L-9619
9. Performing Organization Name and Address NASA Langley Research Center Hampton, Va. 23665		10. Work Unit No. 501-26-04-02
		11. Contract or Grant No.
12. Sponsoring Agency Name and Address National Aeronautics and Space Administration Washington, D.C. 20546		13. Type of Report and Period Covered Technical Note
		14. Sponsoring Agency Code
15. Supplementary Notes		

16. Abstract

A parameter-extraction algorithm was used to determine the lateral aerodynamic derivatives from flight data for the F-8 aircraft with supercritical wing. The flight data used were the recorded responses to aileron or rudder pulses for Mach numbers of 0.80, 0.90, and 0.98.

Results of this study showed that a set of derivatives were determined which yielded a calculated aircraft response almost identical with the response measured in flight. Derivatives extracted from motion resulting from rudder inputs were somewhat different from those resulting from aileron inputs. It was found that the derivatives obtained from the rudder-input data were highly correlated in some instances. Those from the aileron input had very low correlations and appeared to be the more reliable.

17. Key Words (Suggested by Author(s))	18. Distribution Statement
Parameter extraction Maximum likelihood Lateral aerodynamic coefficients	Unclassified – Unlimited STAR Category 02

19. Security Classif. (of this report)	20. Security Classif. (of this page)	21. No. of Pages	22. Price*
Unclassified	Unclassified	35	$3.25

*For sale by the National Technical Information Service, Springfield, Virginia 22151

EXTRACTION FROM FLIGHT DATA OF LATERAL AERODYNAMIC COEFFICIENTS FOR F-8 AIRCRAFT WITH SUPERCRITICAL WING

By James L. Williams and William T. Suit
Langley Research Center

SUMMARY

A parameter-extraction algorithm was used to determine the lateral aerodynamic derivatives from flight data for the F-8 aircraft with supercritical wing. The flight data used were the recorded responses to aileron or rudder pulses for Mach numbers of 0.80, 0.90, and 0.98.

Results of this study showed that a set of derivatives were determined which yielded a calculated aircraft response almost identical with the response measured in flight. Derivatives extracted from motion resulting from rudder inputs were somewhat different from those resulting from aileron inputs. It was found that the derivatives obtained from the rudder-input data were highly correlated in some instances. Those from the aileron input had very low correlations and appeared to be the more reliable.

INTRODUCTION

Analytical and simulator studies of the flight and handling qualities of aircraft require that accurate estimates of the aerodynamic parameters be used if the results are to be valid. To provide aerodynamic parameters for analytical and simulator studies and also to provide numerical values for comparison with wind-tunnel data and theoretical estimates, parameters have been extracted from flight data for many years. Results from recent Langley Research Center investigations in which the aerodynamic parameters for several aircraft have been extracted from flight data are reported in references 1 to 5.

Various techniques for data extraction are presented in reference 6. The technique and program used in extracting the parameters in this study is the maximum likelihood method of reference 7.

The purpose of the present study is to extract static and dynamic lateral aerodynamic parameters from flight tests of the F-8 supercritical-wing aircraft at Mach numbers of 0.80, 0.90, and 0.98. The flight-test data used for the analysis consisted of airplane responses to aileron or rudder pulses.

SYMBOLS

a_Y	acceleration measured along Y body axis, g units
b	wing span, m
$DA = \delta_a - \delta_{a,t}$, rad	
$DR = \delta_r - \delta_{r,t}$, rad	
g	gravitational acceleration, 9.81 m/sec^2
h_p	pressure altitude, m
I_X, I_Y, I_Z	moment of inertia about roll, pitch, and yaw axis, respectively, kg-m^2
I_{XZ}	product of inertia, kg-m^2
l_h	distance from aircraft center of gravity to quarter-chord point of mean geometric chord of horizontal tail, m
M	Mach number
N	number of data points
p	roll rate, rad/sec
q	pitch rate, rad/sec

$R_{a_Y} = \frac{1}{W_{a_Y}}$

$R_p = \frac{1}{W_p}$

$R_r = \frac{1}{W_r}$

$R_v = \frac{1}{W_v}$

$R_{\varphi} = \frac{1}{W_{\varphi}}$

r	yaw rate, rad/sec
S	wing area, m^2
u	velocity component along X body axis, m/sec
V	resultant velocity, m/sec
v	velocity component along Y body axis, m/sec
W	weight, N
$W_{a_Y}, W_p, W_r, W_v, W_{\varphi}$	weighting values of a_Y, p, r, v, and φ state variables
w	velocity component along Z body axis, m/sec
X,Y,Z	body-axis system (see fig. 1)
x	vector of aircraft states
α	angle of attack, deg or rad
β	angle of sideslip, deg or rad
δ_a	aileron deflection, total deflection of left and right ailerons, positive deflection indicates positive roll, deg or rad
δ_r	rudder deflection, positive trailing edge left, deg or rad
θ	pitch attitude, deg or rad
ρ	mass density of air, kg/m^3
φ	roll attitude, rad

Subscripts:

c computed

m measured in flight

t trim

Aerodynamic parameters:

C_l rolling-moment coefficient about X body axis

$C_{l_p} = \frac{\partial C_l}{\partial\left(\frac{pb}{2V}\right)}$

$C_{l_r} = \frac{\partial C_l}{\partial\left(\frac{rb}{2V}\right)}$

$C_{l_\beta} = \frac{\partial C_l}{\partial \beta}$ per radian

$C_{l_{\delta_a}} = \frac{\partial C_l}{\partial \delta_a}$ per radian

$C_{l_{\delta_r}} = \frac{\partial C_l}{\partial \delta_r}$ per radian

C_n yawing-moment coefficient about Z body axis

$C_{n_p} = \frac{\partial C_n}{\partial\left(\frac{pb}{2V}\right)}$

$C_{n_r} = \frac{\partial C_n}{\partial\left(\frac{rb}{2V}\right)}$

$C_{n_\beta} = \frac{\partial C_n}{\partial \beta}$ per radian

$C_{n_{\delta_a}} = \frac{\partial C_n}{\partial \delta_a}$ per radian

$C_{n_{\delta_r}} = \frac{\partial C_n}{\partial \delta_r}$ per radian

C_Y lateral-force coefficient along Y body axis

$C_{Y_p} = \frac{\partial C_Y}{\partial\left(\frac{pb}{2V}\right)}$

$C_{Y_r} = \frac{\partial C_Y}{\partial\left(\frac{rb}{2V}\right)}$

$C_{Y_\beta} = \frac{\partial C_Y}{\partial \beta}$ per radian

$C_{Y_{\delta_a}} = \frac{\partial C_Y}{\partial \delta_a}$ per radian

$C_{Y_{\delta_r}} = \frac{\partial C_Y}{\partial \delta_r}$ per radian

The dot over a symbol denotes rate of change with respect to time.

EQUATIONS OF MOTION

The equations of motion used in this study are referred to a body-axis system (fig. 1) and are as follows:

Y-direction:

$$\dot{v} = pw - ru + g \cos \theta \sin \varphi + \frac{1}{2}\rho V^2 S \frac{g}{W}\left[C_{Y,t} + C_{Y_\beta}(\beta - \beta_t) + C_{Y_p}\frac{pb}{2V} + C_{Y_r}\frac{rb}{2V} + C_{Y_{\delta_r}}(\delta_r - \delta_{r,t}) + C_{Y_{\delta_a}}(\delta_a - \delta_{a,t})\right] \tag{1}$$

Rolling:

$$\dot{p} = -qr\frac{I_Z - I_Y}{I_X} + (pq + \dot{r})\frac{I_{XZ}}{I_X} + \frac{1}{2}\frac{\rho V^2 Sb}{I_X}\left[C_{l,t} + C_{l_\beta}(\beta - \beta_t) + C_{l_p}\frac{pb}{2V} + C_{l_r}\frac{rb}{2V} + C_{l_{\delta_r}}(\delta_r - \delta_{r,t}) + C_{l_{\delta_a}}(\delta_a - \delta_{a,t})\right] \tag{2}$$

Yawing:

$$\dot{r} = -pq\frac{I_Y - I_X}{I_Z} - (qr - \dot{p})\frac{I_{XZ}}{I_Z} + \frac{1}{2}\frac{\rho V^2 Sb}{I_Z}\left[C_{n,t} + C_{n_\beta}(\beta - \beta_t) + C_{n_p}\frac{pb}{2V}\right.$$

$$\left. + C_{n_r}\frac{rb}{2V} + C_{n_{\delta_a}}(\delta_a - \delta_{a,t}) + C_{n_{\delta_r}}(\delta_r - \delta_{r,t})\right] \tag{3}$$

Auxiliary equations:

$$\alpha = \tan^{-1}\frac{w}{u}$$

$$\beta = \sin^{-1}\frac{v}{V}$$

$$a_Y = \frac{1}{g}(\dot{v} + ur - wp - g\cos\theta\sin\varphi)$$

The three-degree-of-freedom lateral equations (eqs. (1) to (3)) were solved for the lateral motions. The longitudinal state variables u, w, and q used in these equations were the flight-measured values, and hence the nonlinear contributions of these terms were used in the equations.

DESCRIPTION OF AIRPLANE

The aerodynamic parameters were extracted from data obtained from an F-8 aircraft on which the original wing was replaced with a supercritical wing which is described in reference 8. The F-8 is a single-seat high performance airplane with a single jet engine embedded in the fuselage and with an all-movable horizontal tail. Figure 2 is a photograph of the airplane. Pertinent geometric characteristics of the airplane are given in table I.

Flight instrumentation appropriate to this study included the following items:

(1) Roll-, pitch-, and yaw-rate gyros

(2) Angle-of-attack indicator

(3) Angle-of-sideslip indicator

(4) Altimeter

(5) Total velocity indicator

(6) Aileron and rudder position indicators

(7) Magnetic tape recorders

(8) Accelerometers

(9) Pitch- and roll-angle gyros

The full-scale range of the flight instruments and their accuracies are given in table II.

FLIGHT TESTS

The data presented in this study were obtained from in-flight measurement of the airplane response to aileron or rudder inputs. These flights were made at the NASA Flight Research Center as part of a general evaluation program of the F-8 supercritical-wing aerodynamics.

Data were obtained at Mach numbers of 0.80, 0.90, and 0.98. The control inputs used to generate the lateral motions (three degrees of freedom) were one or more aileron or rudder pulses. All data used in this study for parameter extraction were reduced at Flight Research Center and have been corrected for bias and displacement of the measuring instrument from the aircraft center of gravity. Test conditions and mass characteristics are presented in table III.

PARAMETER-EXTRACTION PROCEDURE

The parameter-extraction procedure used in this study is an iterative technique which utilizes the maximum likelihood method to extract the stability and control parameters. (See ref. 7 for details of the method.) This method maximizes the conditional likelihood L which is a function of aerodynamic parameters, weights, and initial conditions:

$$L = \frac{1}{(2\pi)^{1/2}R^{1/2}} \exp\left[-\frac{1}{2}\sum_{i=1}^{N}(x_{i,m} - x_{i,c})^T R^{-1}(x_{i,m} - x_{i,c})\right]$$

where R is the estimate of the error covariance matrix and x is a vector describing the state of the aircraft. Maximization of the likelihood function L provides the following information:

(1) The parameter increments which are used to update the parameter

(2) The covariance matrices whose elements are proportional to the estimated standard deviations and the pairwise correlation coefficients for the parameters and for the states

(3) The performance index function J which is an indicator of the fit between measured and calculated motion

The interative technique produces a set of estimated derivatives which, when used in the equations of motion (eqs. (1) to (3)), provide the best fit to the time variation of the aircraft motion measured in flight. The criterion for the best fit is the performance index J which is defined as

$$J = \det\left[\frac{1}{N}\sum_{i=1}^{N}(x_{i,m} - x_{i,c})(x_{i,m} - x_{i,c})^T\right]$$

where det denotes determinant and x is the vector describing the state of the aircraft. Generally, the performance index J becomes smaller with sucessive iterations. The iteration procedure is stopped when the value of J does not change appreciably for several successive iterations.

The components of the vector x are the state variables v, p, r, φ, and a_Y which are calculated from equations (1) to (3). The quantities u_m, v_m, and w_m were not measured directly but were obtained from the measured total velocity, angle of sideslip, and angle of attack through the use of the following equations:

$$u_m = V_m \cos \alpha_m \cos \beta_m$$

$$v_m = V_m \sin \beta_m$$

$$w_m = V_m \cos \beta \sin \alpha_m$$

Maximization of the likelihood function yields the covariance matrix for the measurement noise based on the current solution. (See ref. 7.) This matrix gives the variances (or standard deviations) of the differences of the measured state and the current solution. The inverse of this matrix is the weighting matrix used in the parameter-change equations. In this investigation, the diagonal form of the weighting matrix was used and the diagonal elements can be expressed as the squares of the differences between the measured and calculated data. For example, the weight for the state variable v is expressed as

$$\frac{1}{R_v^2} = \frac{1}{N}\sum_{i=1}^{N}(v_m - v_c)_i^2$$

Similar equations are obtained for the other state variables used in the cost function $\left(1/R_p^2,\ 1/R_r^2,\ 1/R_{a_Y}^2, \text{ and } 1/R_\varphi^2\right)$.

Initial values of the state variables were obtained from the flight records for the time period prior to a control input. Initial values of the aerodynamic derivatives (table IV) were obtained from a preliminary investigation in the Langley 8-foot transonic pressure tunnel for $\alpha = 4^\circ$. Although the tabulated derivatives were for a Mach number of 0.8, they were used as initial values for all the work presented herein. The data rate for the in-flight measurements was 25 points per second.

RESULTS AND DISCUSSION

Measured and calculated time histories are compared in figures 3 to 6. The calculated motions are those obtained after the parameter-extraction program had converged on a set of derivatives for each flight condition. Figures 3 and 4 show the responses to rudder inputs for flight at a Mach number of 0.80 and 0.90, respectively. Figures 5 and 6 are responses to aileron inputs for a Mach number of 0.90 and 0.98, respectively. In all cases, the calculated time histories match the flight results very closely. The standard deviations of the converged states are given in table V.

The aerodynamic parameters extracted for each of the four flight conditions in figures 3 to 6 are listed in table VI. Also shown in the table are the estimates of the standard deviations of the parameters. The standard deviations are generally less than 10 percent of the extracted derivative, which implies that the extracted derivatives are well defined. Most of the derivatives are of reasonable magnitude and are close to the initial values shown in table IV. However, a comparison of derivatives for the rudder-input and the aileron-input cases at the same Mach number (M = 0.90) shows appreciable differences in some derivatives, for example, C_{l_β}, C_{l_p}, and C_{l_r}. The difference in C_{l_r} was particularly bothersome since there was a sign difference. In order to determine if this discrepancy was caused by differences in control input or for some other reason, the correlation matrices for each set of extracted derivatives were examined. The correlation matrices are shown as tables VII (aileron input) and VIII (rudder input). It is apparent that several high correlations exist for the rudder-input case, whereas the correlations are quite low for the aileron-input case. It appeared, therefore, that the derivatives from the aileron-input time histories were more reliable than those from the rudder-input cases. In order to check this possibility, the aerodynamic derivatives that had been extracted from the rudder-input flight data were used to calculate motions for the aileron-input case. The results are presented in figure 7 and show poor agreement with flight data. Motions were then calculated for the rudder-input case from the aerodynamic parameters extracted from the aileron-input data. The results, shown in figure 8, show good agreement with the flight data. The conclusion, therefore, is that the derivatives extracted from the aileron-input data are more reliable than those from the rudder-input data. The precise reason for the superiority of an aileron input over a rudder input in obtaining good, uncorrelated aerodynamic parameters is not known at this time, and is a subject for future study. As a matter of interest, the derivatives from the aileron-input case were used as initial values for the rudder-input flight (which resulted in the comparison of fig. 8), and the parameter-extraction program was permitted to iterate. After several iterations the fit to the data improved, and the extracted parameters converged to the values of the derivatives of table VI for the rudder input.

The negative values of C_{l_r} extracted from the aileron-input data, theoretically, should have been positive. It was believed that perhaps the time histories were insensitive to C_{l_r}; therefore, several computations were made for the rudder-input case with $M = 0.9$ for all derivatives fixed at the values of table VI except C_{l_r}. The results are shown in figure 9, and indicate that the effect of varying C_{l_r} is quite noticeable.

Some of the extracted parameters of table VI are compared with wind-tunnel values in table IX. In general, the agreement is reasonably good; however, there are some appreciable differences between the flight-extracted and wind-tunnel values. The most obvious difference is the large variance between the extracted and wind-tunnel values for $C_{n_{\delta_r}}$. One reason for this is possibly aeroelastic effects. Since rigid body equations of motion were used in the extraction algorithm, the effect of aeroelasticity on the extracted parameters was not considered in this study.

CONCLUDING REMARKS

A parameter-extraction algorithm was used to determine the lateral aerodynamic derivatives from flight data for the F-8 aircraft with supercritical wing. The flight data were the responses to aileron or rudder pulses for Mach numbers of 0.80, 0.90, and 0.98.

Results of this study showed that a set of derivatives were determined which yielded a calculated aircraft response almost identical with the response measured in flight. Derivatives extracted from motion resulting from rudder inputs were somewhat different from those resulting from aileron inputs. It was found that the derivatives obtained from the rudder-input data were highly correlated in some instances. Those from the aileron input had very low correlations and appeared to be the more reliable in fitting the measured responses.

Langley Research Center,
National Aeronautics and Space Administration,
Hampton, Va., August 12, 1974.

REFERENCES

1. Suit, William T.: Aerodynamic Parameters of the Navion Airplane Extracted From Flight Data. NASA TN D-6643, 1972.
2. Steinmetz, George G.; Parrish, Russell V.; and Bowles, Roland L.: Longitudinal Stability and Control Derivatives of a Jet Fighter Airplane Extracted From Flight Test Data by Utilizing Maximum Likelihood Estimation. NASA TN D-6532, 1972.
3. Williams, James L.: Extraction of Longitudinal Aerodynamic Coefficients From Forward-Flight Conditions of a Tilt-Wing V/STOL Airplane. NASA TN D-7114, 1972.
4. Suit, William T.; and Williams, James L.: Longitudinal Aerodynamic Parameters of the Kestrel Aircraft (XV-6A) Extracted From Flight Data. NASA TN D-7296, 1973.
5. Williams, James L.; and Suit, William T.: Extraction From Flight Data of Longitudinal Aerodynamic Coefficients for F-8 Aircraft With Supercritical Wing. NASA TN D-7470, 1974.
6. Denery, Dallas G.: Identification of System Parameters From Input-Output Data With Application to Air Vehicles. NASA TN D-6468, 1971.
7. Grove, Randall D.; Bowles, Roland L.; and Mayhew, Stanley C: A Procedure for Estimating Stability and Control Parameters From Flight Test Data by Using Maximum Likelihood Methods Employing a Real-Time Digital System. NASA TN D-6735, 1972.
8. Bartlett, Dennis W.; and Re, Richard J.: Wind-Tunnel Investigation of Basic Aerodynamic Characteristics of a Supercritical-Wing Research Airplane Configuration. NASA TM X-2470, 1972.

TABLE I.- GEOMETRIC CHARACTERISTICS OF F-8 AIRCRAFT WITH SUPERCRITICAL WING

Fuselage:	
Length, m	16.09
Wing:	
Area, m^2	25.45
Aspect ratio	6.77
Span, m	13.14
Mean geometric chord, m	2.08
Vertical tail:	
Area, m^2	10.13
Aspect ratio	1.5
Span, m	3.88
Rudder:	
Area, m^2	1.17
Horizontal tail:	
Area, m^2	8.68
Aspect ratio	3.5
Span, m	5.52
Tail length, center of gravity to quarter-chord point of mean geometric chord, m	5.31

TABLE II.- INSTRUMENT RANGES AND ACCURACIES

Measured quantities	Range	Accuracy
Angle of attack, deg	-5 to 25	±0.3
Pressure altitude, m	0 to 18 000	±11
Total velocity, m/sec	0 to 360	±0.7
Lateral acceleration at c.g., g units	±1.0	±0.01
Longitudinal acceleration at c.g., g units	±0.5	±0.01
Roll angle, deg	±90	±1.8
Pitch angle, deg	±30	±0.6
Roll rate, deg/sec	±200	±0.6
Pitch rate, deg/sec	±40	±0.8
Yaw rate, deg/sec	±12	±0.3
Rudder position, deg	±8	±0.3
Aileron position, deg	±15	±0.8

TABLE III.- TEST CONDITIONS AND MASS CHARACTERISTICS

	M = 0.80	M = 0.90	M = 0.98
Weight, N	100 802	104 912	101 792
Mass, kg	10 279.1	10 698.2	10 380.0
I_X, kg-m^2	20 484	20 512	20 491
I_Y, kg-m^2	124 383	125 350	124 616
I_Z, kg-m^2	138 424	139 363	138 650
I_{XZ}, kg-m^2	4359	4522	4399
h_p, m	12 178	12 751	13 862
l_h, m	5.31	5.30	5.27

TABLE IV.- INITIAL VALUES OF AERODYNAMIC DERIVATIVES

C_{Y_β}	-1.317
C_{l_β}	-0.234
C_{l_p}	-0.390
$C_{l_{\delta_a}}$	0.069
C_{n_r}	-0.492
$C_{n_{\delta_a}}$	-0.005
C_{l_r}	0.231
C_{n_p}	-0.183
C_{n_β}	0.148

TABLE V.- STANDARD DEVIATIONS OF CONVERGED STATES

M	Input	Standard deviation of –				
		v, m/sec	p, rad/sec	r, rad/sec	φ, rad	a_Y, g
0.80	Rudder	0.4095	0.0036	0.0010	0.0018	0.0036
.90	Rudder	.3041	.0065	.0026	.0045	.0046
.90	Aileron	.3080	.0085	.0011	.0091	.0044
.98	Aileron	.3326	.0165	.0028	.0163	.0067

TABLE VI.- EXTRACTED AERODYNAMIC PARAMETERS AND STANDARD DEVIATIONS

Parameters	Parameters and standard deviations[a] for –			
	Rudder input		Aileron input	
	M = 0.80	M = 0.90	M = 0.90	M = 0.98
$C_{Y,t}$	-0.01597	-0.0172	0.0014	-0.0171
	(0.000149)	(0.00013)	(0.00017)	(0.00017)
C_{Y_β}	-1.2063	-1.2055	-1.2283	-1.1868
	(0.009819)	(0.0086)	(0.0209)	(0.02363)
$C_{Y_{\delta_r}}$	0.03182	0.0325	0.0320	0.0320
	(0.001093)	(0.00127)	(Fixed)	(Fixed)
$C_{Y_{\delta_a}}$	0	0	-0.0228	-0.01342
	0	0	(0.00357)	(0.00325)
$C_{l,t}$	-0.000202	0.00051	-0.00053	-0.00034
	(0.000012)	(0.000013)	(0.00002)	(0.00002)
C_{l_β}	-0.23399	-0.2052	-0.2748	-0.2751
	(0.00200)	(0.00174)	(0.0018)	(0.00284)
C_{l_p}	-0.4948	-0.3928	-0.5938	-0.6867
	(0.00614)	(0.00529)	(0.0044)	(0.00743)
C_{l_r}	0.2111	1.5767	-0.4546	-0.4749
	(0.03553)	(0.03256)	(0.0342)	(0.0887)
$C_{l_{\delta_r}}$	0.0046	0.0063	0.005	0.005
	(0.000069)	(0.000075)	(Fixed)	(Fixed)
$C_{l_{\delta_a}}$	0.0940	0.0940	0.0941	0.0740
	(Fixed)	(Fixed)	(0.00051)	(0.00062)
$C_{n,t}$	-0.000093	-0.00028	0.00022	0.00000
	(0.000007)	(0.000009)	(0.00001)	(0.000009)
C_{n_β}	0.1449	0.1552	0.1473	0.1334
	(0.000901)	(0.00091)	(0.00041)	(0.00069)
C_{n_p}	0.02292	0.00796	-0.0059	-0.0360
	(0.002674)	(0.0026)	(0.00166)	(0.00311)
C_{n_r}	-0.20581	-0.31961	-0.4368	-0.6057
	(0.02029)	(0.0230)	(0.01051)	(0.0241)
$C_{n_{\delta_r}}$	-0.01481	-0.01526	-0.015	-0.0150
	(0.000047)	(0.000059)	(Fixed)	(Fixed)
$C_{n_{\delta_a}}$	-0.0022	-0.0022	-0.0022	-0.0024
	(Fixed)	(Fixed)	(0.00019)	(0.00026)

[a]Standard deviations are given in parentheses.

TABLE VII.- ESTIMATED PAIRWISE CORRELATION COEFFICIENTS AT CONVERGENCE FOR AILERON INPUT AT $M = 0.90$

	$C_{Y,t}$	C_{Y_β}	$C_{l,t}$	C_{l_β}	C_{l_p}	C_{l_r}	$C_{l_{\delta_a}}$	$C_{n,t}$	C_{n_β}	C_{n_p}	C_{n_r}	$C_{n_{\delta_a}}$	$C_{Y_{\delta_a}}$
$C_{Y,t}$		0.2233	0.4939	0.0184	-0.0030	-0.0165	-0.0234	-0.4867	0.0378	0.0621	0.0231	0.0037	0.1231
C_{Y_β}	0.2233		0.0395	0.1645	-0.0267	0.1335	0.0333	-0.0066	0.1382	0.1038	-0.2624	-0.1398	0.1067
$C_{l,t}$	0.4939	0.0395		0.1267	0.0942	0.1890	-0.1051	-0.9234	0.1808	0.0695	0.0349	-0.0392	0.0049
C_{l_β}	0.0184	0.1645	0.1267		0.0389	0.0032	-0.0289	0.0822	0.7248	0.1017	-0.0538	-0.3075	0.0514
C_{l_p}	-0.0030	-0.0267	0.0942	0.0389		0.1286	-0.7515	0.0069	0.1806	0.4453	-0.0777	-0.3827	0.0385
C_{l_r}	-0.0165	0.1335	0.1890	0.0032	0.1286		-0.2020	0.0194	-0.0671	-0.2316	-0.2741	-0.0083	0.0330
$C_{l_{\delta_a}}$	-0.0234	0.0333	-0.1051	-0.0289	-0.7515	-0.2020		0.0835	-0.1375	-0.2201	0.0700	0.3329	-0.0022
$C_{n,t}$	-0.4867	-0.0066	-0.9234	0.0822	0.0069	0.0194	0.0835		-0.0142	0.0250	0.0617	-0.0655	-0.0053
C_{n_β}	0.0378	0.1382	0.1808	0.7248	0.1806	-0.0671	-0.1375	-0.0142		0.3301	-0.0571	-0.5035	-0.1326
C_{n_p}	0.0621	0.1038	0.0695	0.1017	0.4453	-0.2316	-0.2201	0.0250	0.3301		0.3638	-0.8135	-0.0486
C_{n_r}	0.0231	-0.2624	0.0349	-0.0538	-0.0777	-0.2741	0.0700	0.0617	-0.0571	0.3638		-0.0811	-0.1010
$C_{n_{\delta_a}}$	0.0037	-0.1398	-0.0392	-0.3075	-0.3827	-0.0083	0.3329	-0.0655	-0.5035	-0.8135	-0.0811		0.0745
$C_{Y_{\delta_a}}$	0.1231	0.1067	0.0049	0.0514	0.0385	0.0330	-0.0022	-0.0053	-0.1326	-0.0486	-0.1010	0.0745	

TABLE VIII.- ESTIMATED PAIRWISE CORRELATION COEFFICIENTS AT CONVERGENCE FOR RUDDER INPUT AT $M = 0.90$

	$C_{Y,t}$	C_{Y_β}	$C_{Y_{\delta_r}}$	$C_{l,t}$	C_{l_β}	C_{l_p}	C_{l_r}	$C_{l_{\delta_r}}$	$C_{n,t}$	C_{n_β}	C_{n_p}	C_{n_r}	$C_{n_{\delta_r}}$
$C_{Y,t}$		-0.1927	-0.1335	0.4530	0.0739	0.0850	0.1423	-0.0559	-0.4872	-0.0710	-0.0815	-0.0425	-0.0297
C_{Y_β}	-0.1927		0.0473	-0.0864	0.1801	0.0475	-0.0225	0.0572	-0.0011	0.1073	0.0740	-0.0445	-0.3749
$C_{Y_{\delta_r}}$	-0.1335	0.0473		-0.0598	0.0195	0.0514	-0.0104	0.0411	0.0495	-0.0142	0.0142	-0.0149	0.0464
$C_{l,t}$	0.4530	-0.0864	-0.0598		-0.2904	-0.2743	-0.1765	-0.2035	-0.9479	0.1990	0.2106	0.2415	-0.0290
C_{l_β}	0.0739	0.1801	0.0195	-0.2904		0.9066	0.8042	0.2937	0.0545	-0.6386	-0.7219	-0.7365	-0.3831
C_{l_p}	0.0850	0.0475	0.0514	-0.2743	0.9066		0.8543	0.2867	0.1167	-0.8282	-0.8709	-0.8779	-0.1188
C_{l_r}	0.1423	-0.0225	-0.0104	-0.1765	0.8042	0.8543		0.4837	0.0203	-0.7681	-0.7653	-0.6989	0.0665
$C_{l_{\delta_r}}$	-0.0559	0.0572	0.0411	-0.2035	0.2937	0.2867	0.4837		0.1000	-0.2576	-0.2234	-0.2406	-0.0312
$C_{n,t}$	-0.4872	-0.0011	0.0495	-0.9479	0.0545	0.1167	0.0203	0.1000		-0.2027	-0.1823	-0.2045	0.1612
C_{n_β}	-0.0710	0.1073	-0.0142	0.1990	-0.6386	-0.8282	-0.7681	-0.2576	-0.2027		0.9838	0.9438	-0.1006
C_{n_p}	-0.0815	0.0740	0.0142	0.2106	-0.7219	-0.8709	-0.7653	-0.2234	-0.1823	0.9838		0.9666	0.0073
C_{n_r}	-0.0425	-0.0445	-0.0149	0.2415	-0.7365	-0.8779	-0.6989	-0.2406	-0.2045	0.9438	0.9666		0.1659
$C_{n_{\delta_r}}$	-0.0297	-0.3749	0.0464	-0.0290	-0.3831	-0.1188	0.0665	-0.0312	0.1612	-0.1006	0.0073	0.1659	

TABLE IX.- COMPARISON OF EXTRACTED DERIVATIVES WITH WIND-TUNNEL RESULTS

Coefficient	M = 0.80		M = 0.90			M = 0.98	
	Wind tunnel	Rudder input	Wind tunnel	Rudder input	Aileron input	Wind tunnel	Aileron input
C_{l_p}	-0.390	-0.495	-0.420	-0.393	-0.594	-0.445	-0.687
C_{n_r}	-.492	-.206	-.583	-.320	-.437	-.601	-.606
C_{n_β}	.148	.145	.166	.155	.147	.206	.133
C_{Y_β} . . .	-1.327	-1.206	-1.450	-1.206	-1.228	-1.501	-1.187
C_{l_β}	-.234	-.234	-.304	-.205	-.275	-.172	-.275
C_{n_p}		.023		.008	-.006	-.010	-.036
$C_{l_{\delta_a}}$ . . .	.069		.069		.094	.069	.074
$C_{n_{\delta_r}}$ . . .	-.183	-.015	-.183	-.015		-.183	

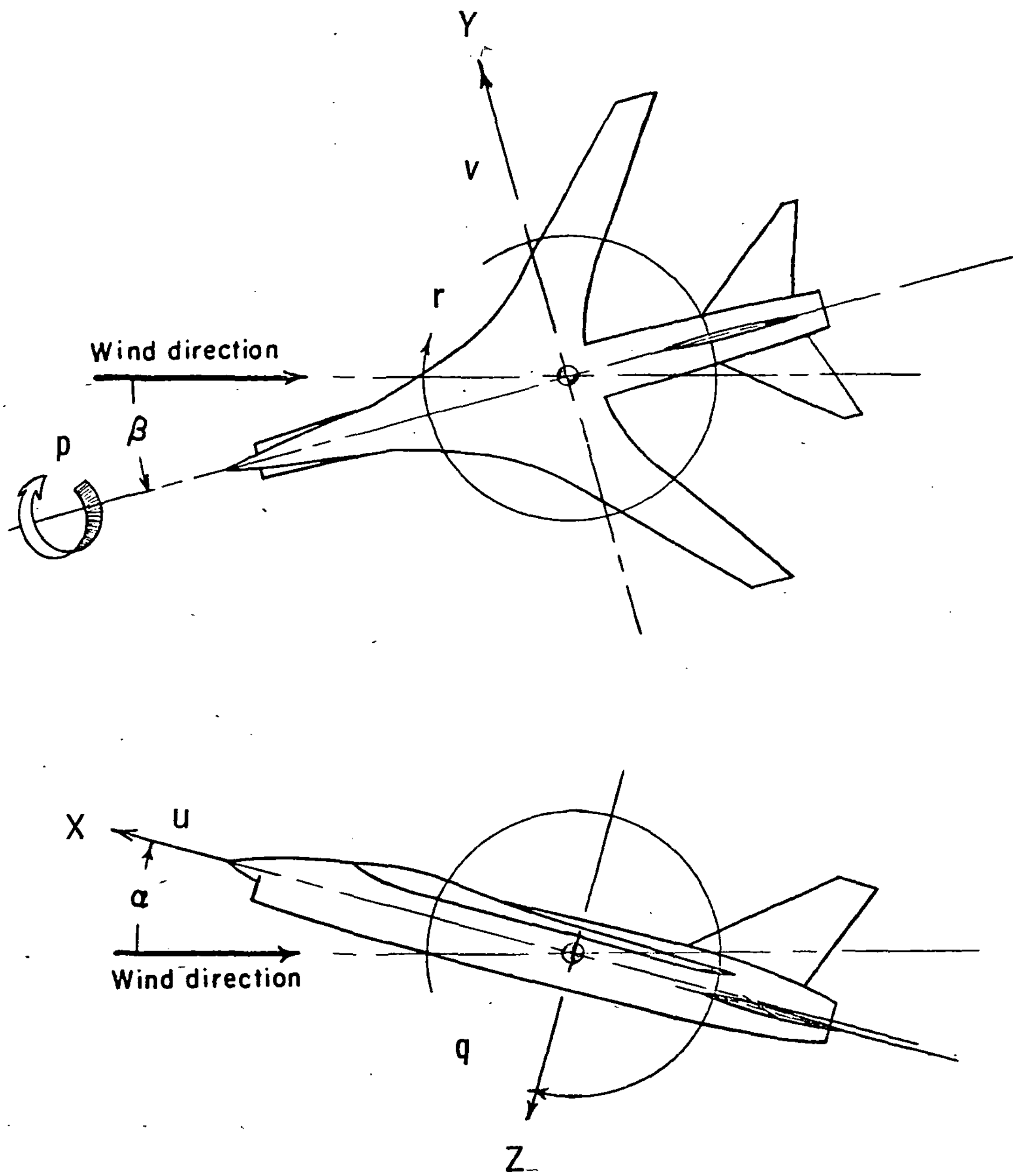

Figure 1.- System of axes. Positive directions of forces, moments, and angles are indicated by arrows.

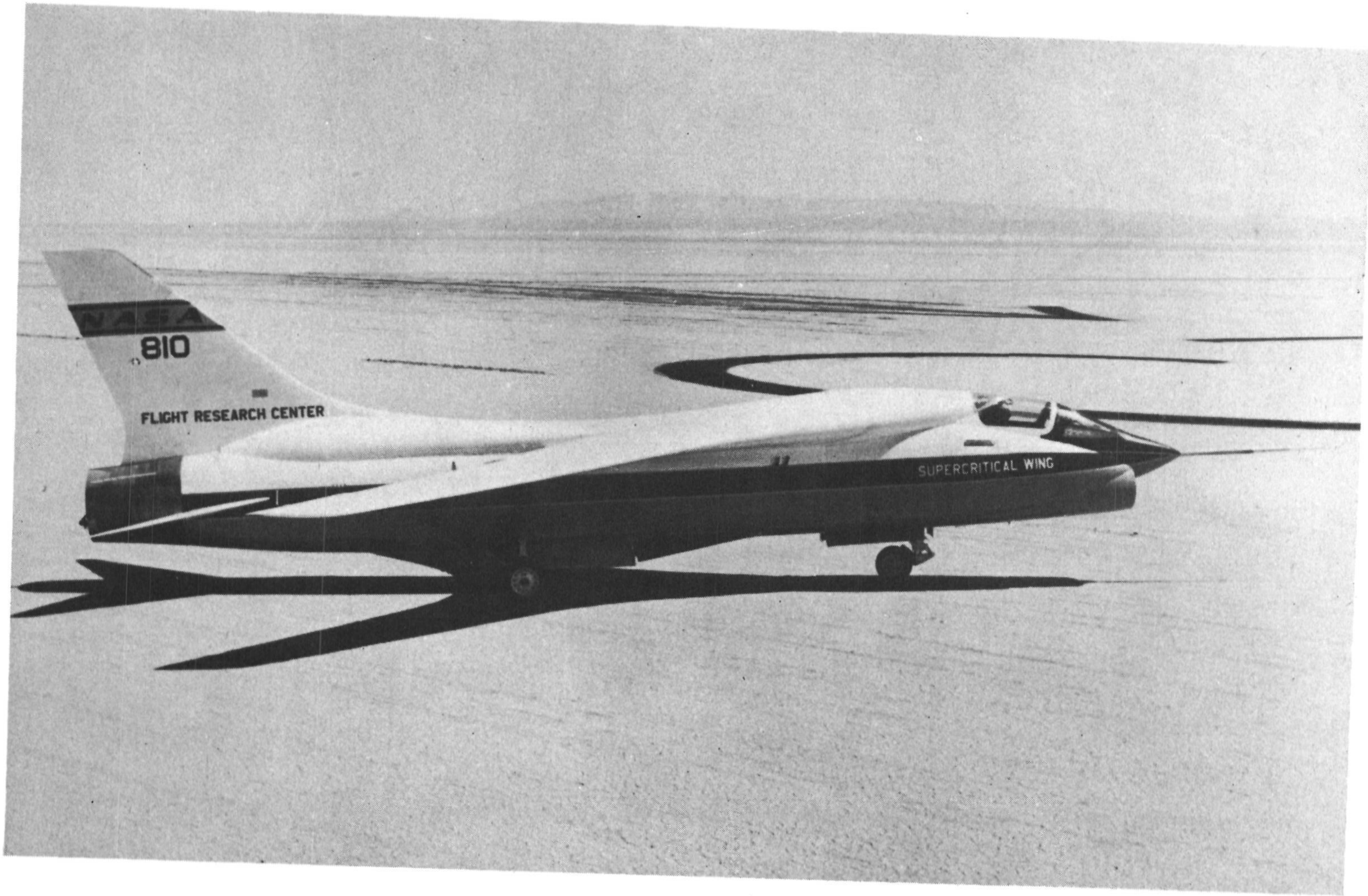

Figure 2.- Aircraft for which derivatives were extracted.

L-72-9010

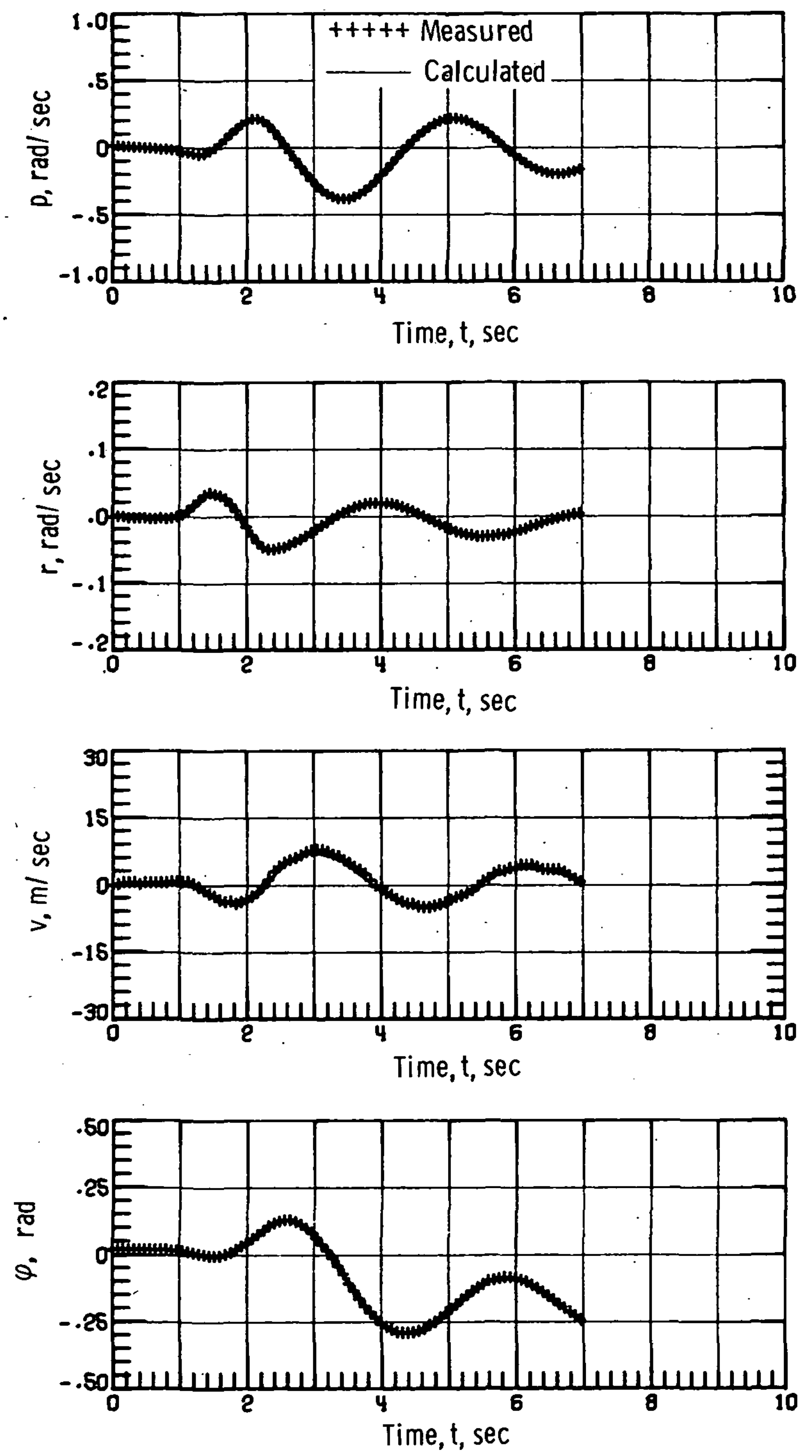

Figure 3.- Comparison of flight data with time histories computed by using the aerodynamic parameters of table VI for rudder input at M = 0.80.

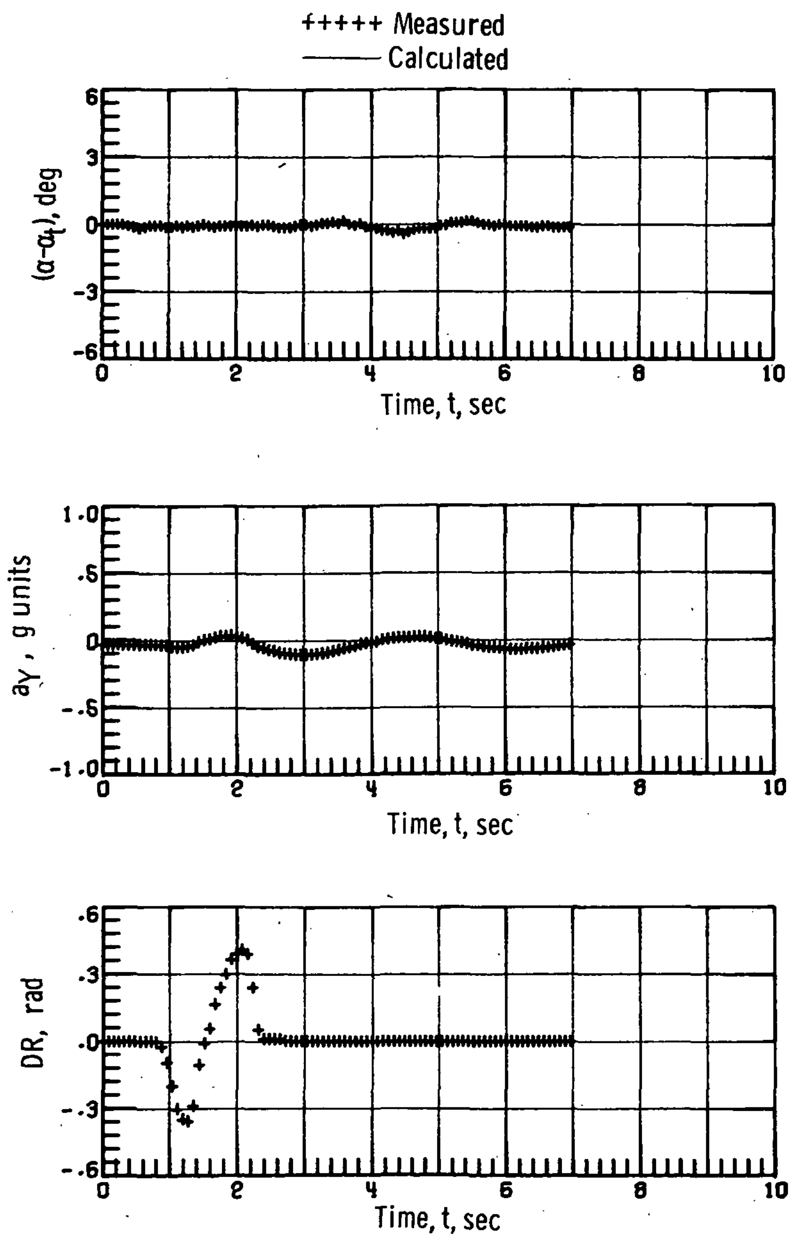

Figure 3.- Concluded.

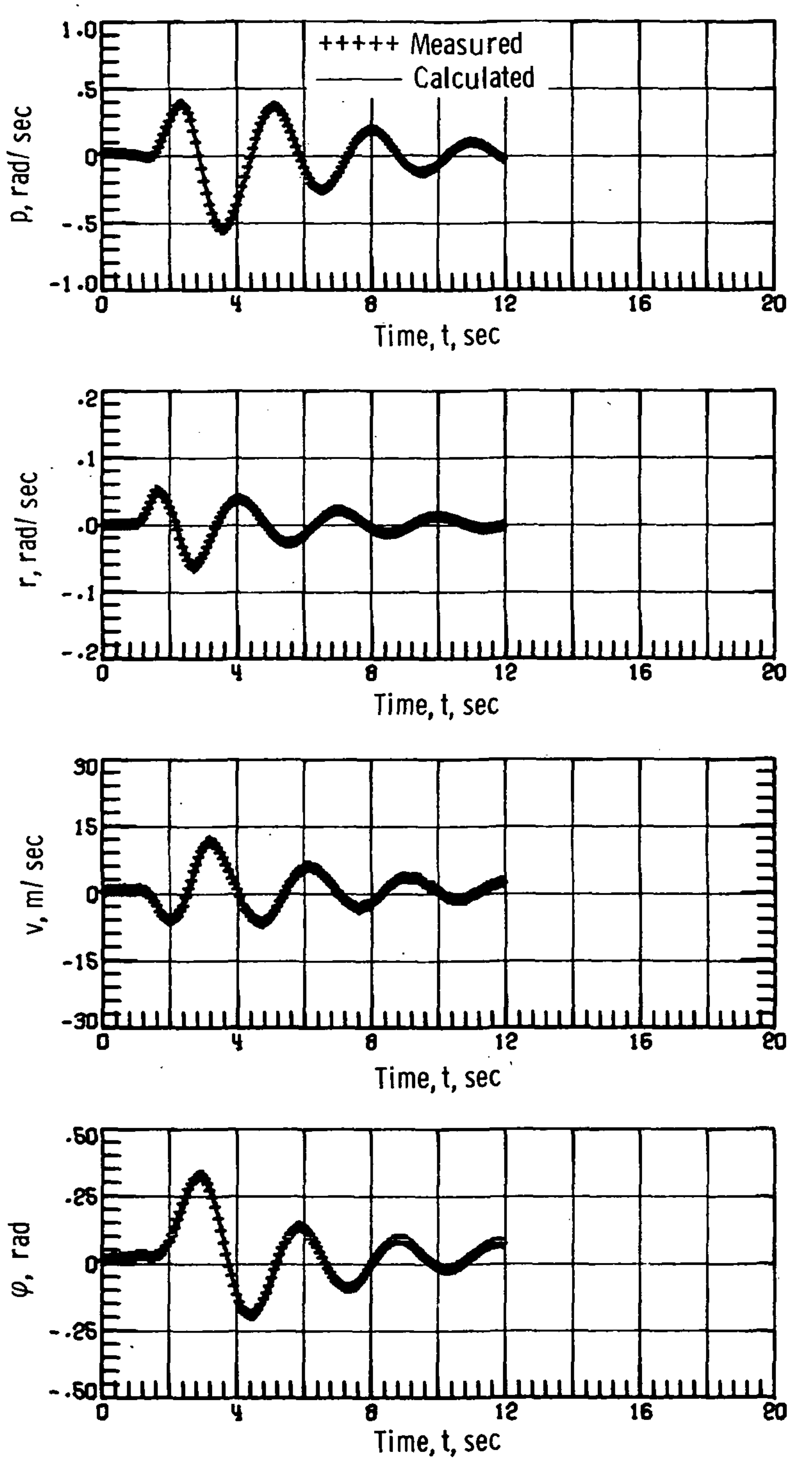

Figure 4.- Comparison of flight data with time histories computed by using the aerodynamic parameters of table VI for rudder input at M = 0.90.

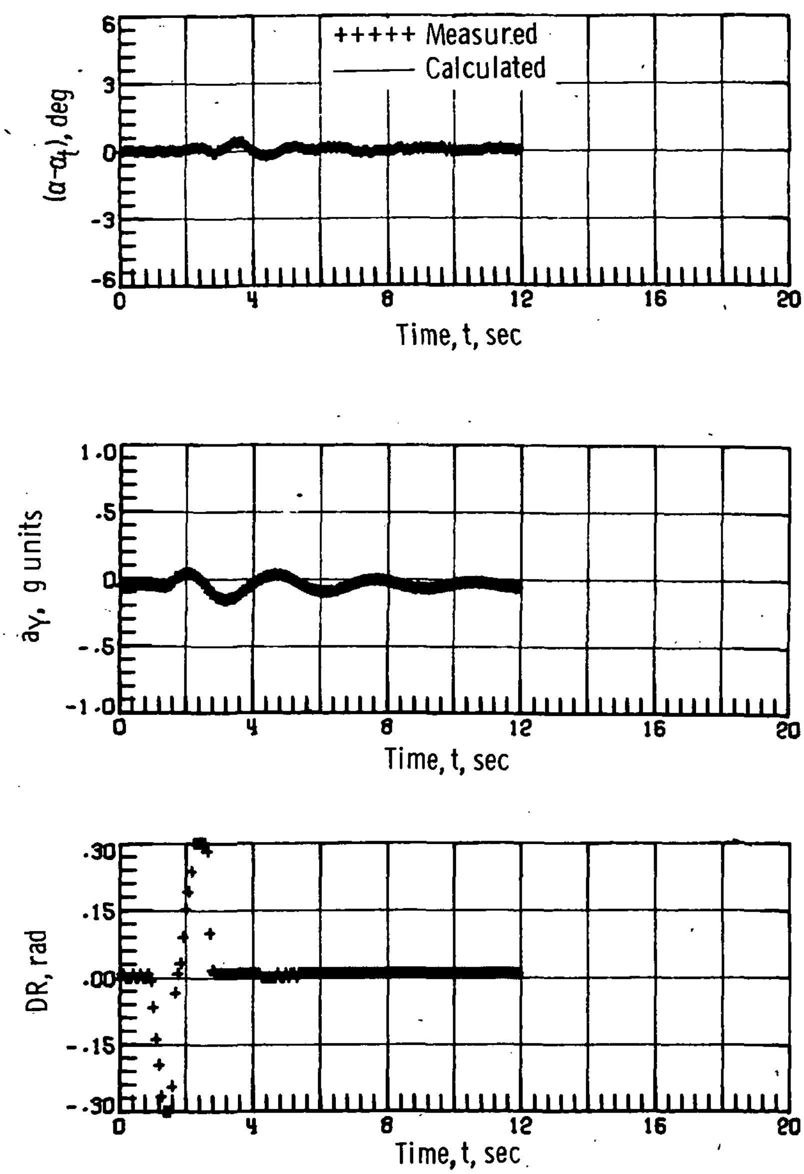

Figure 4.- Concluded.

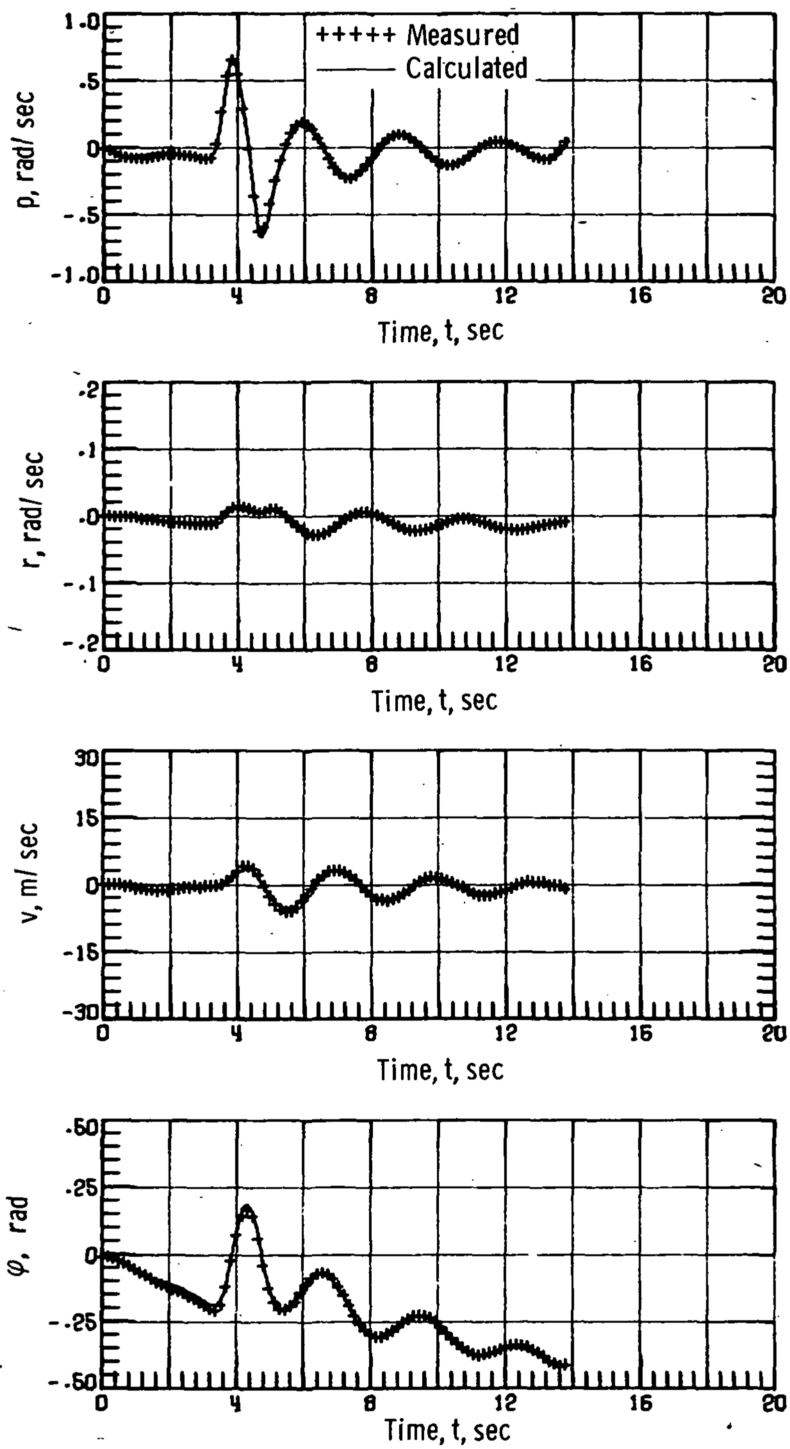

Figure 5.- Comparison of flight data with time histories computed by using the aerodynamic parameters of table VI for aileron inputs at M = 0.90.

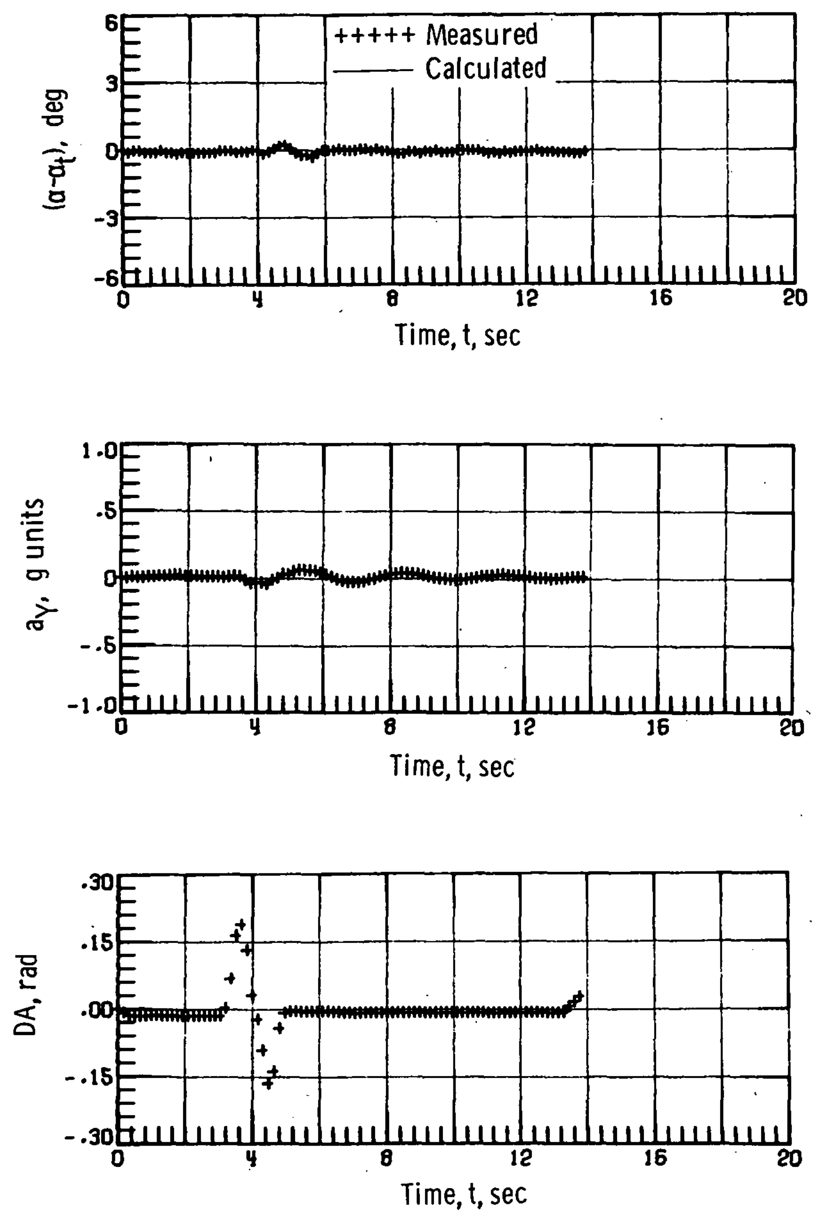

Figure 5.- Concluded.

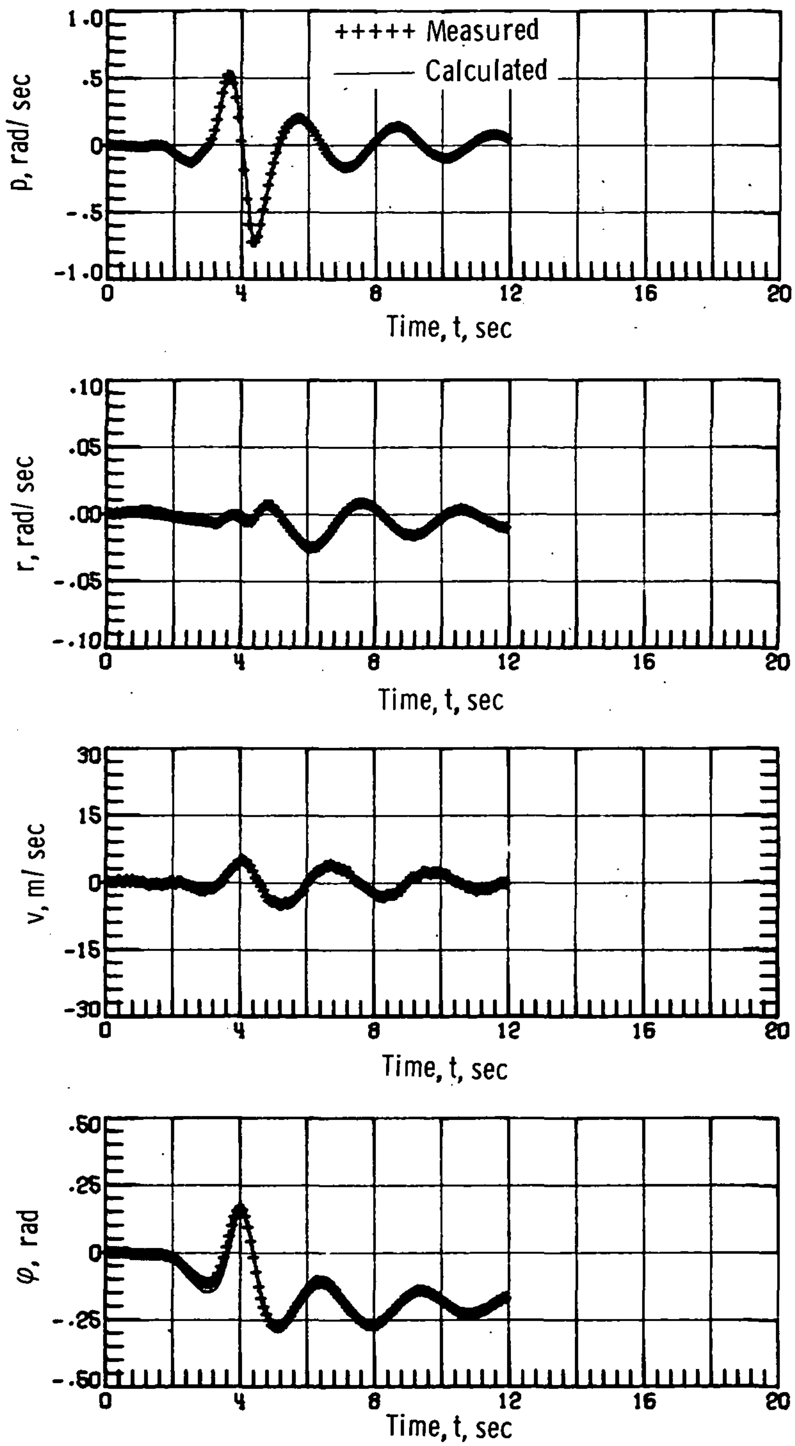

Figure 6.- Comparison of flight data with time histories computed by using the aerodynamic parameters of table VI for aileron input at $M = 0.98$.

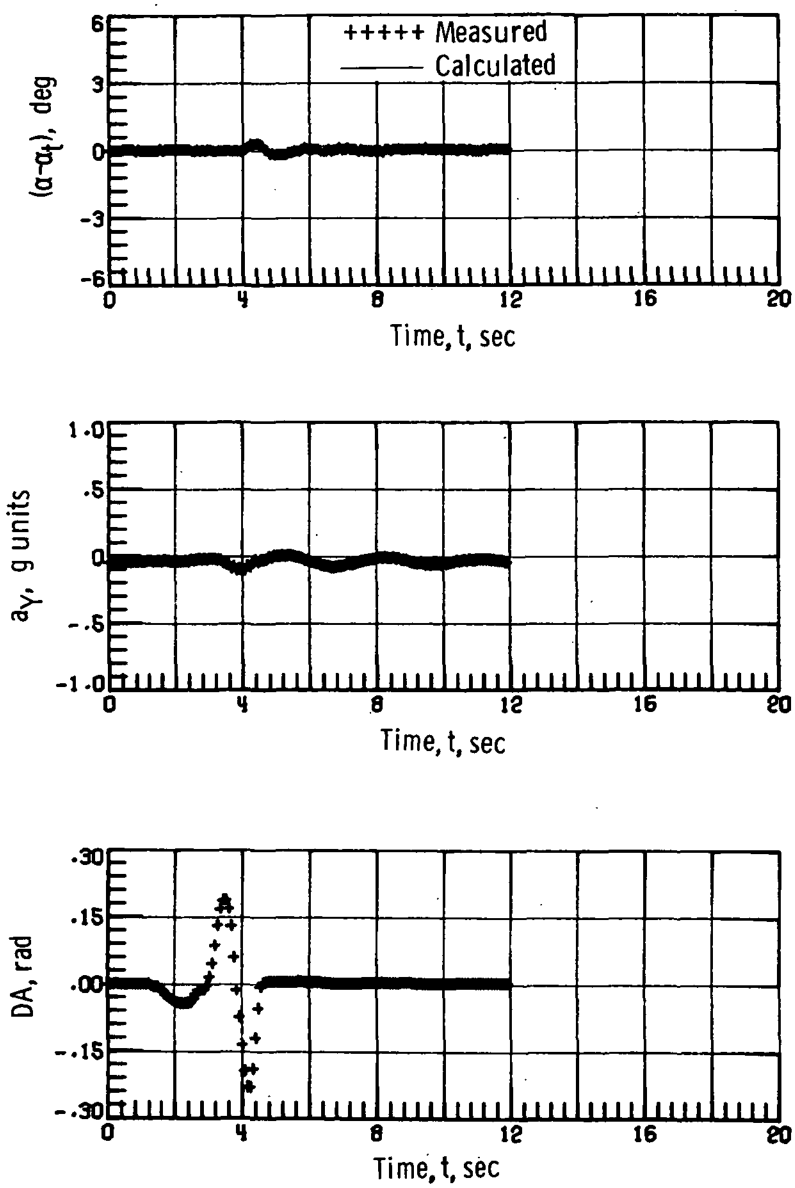

Figure 6.- Concluded.

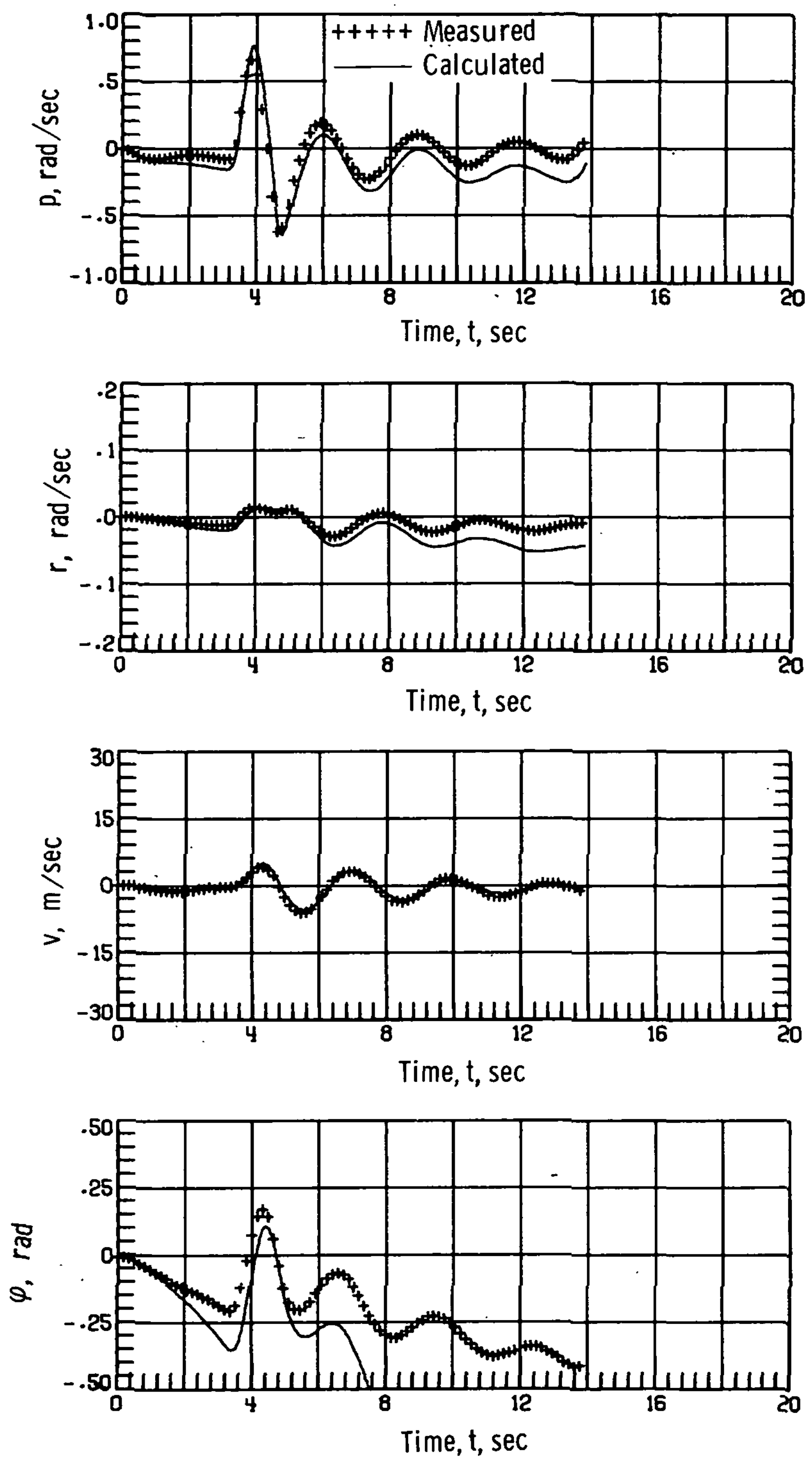

Figure 7.- Comparison of flight data with time histories computed by using the aerodynamic parameters based on rudder induced motions at $M = 0.90$.

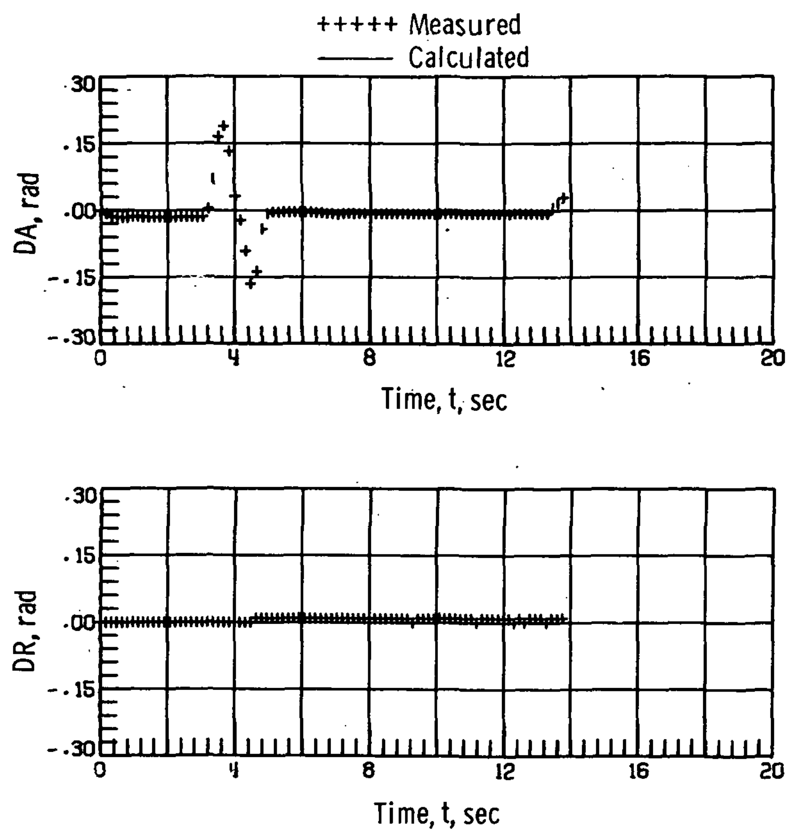

Figure 7.- Concluded.

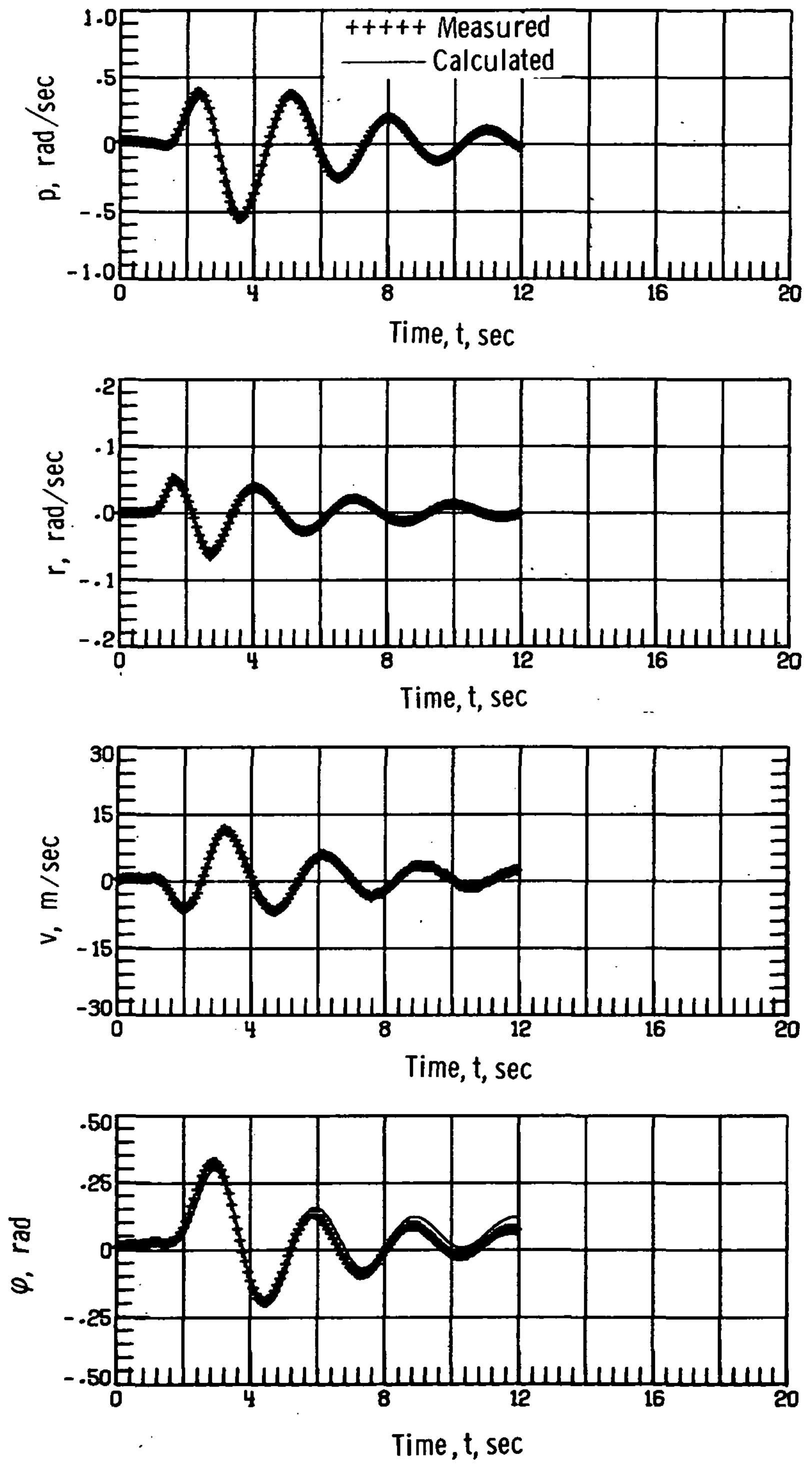

Figure 8.- Comparison of flight data with time histories computed by using the aerodynamic parameters based on aileron control at M = 0.90.

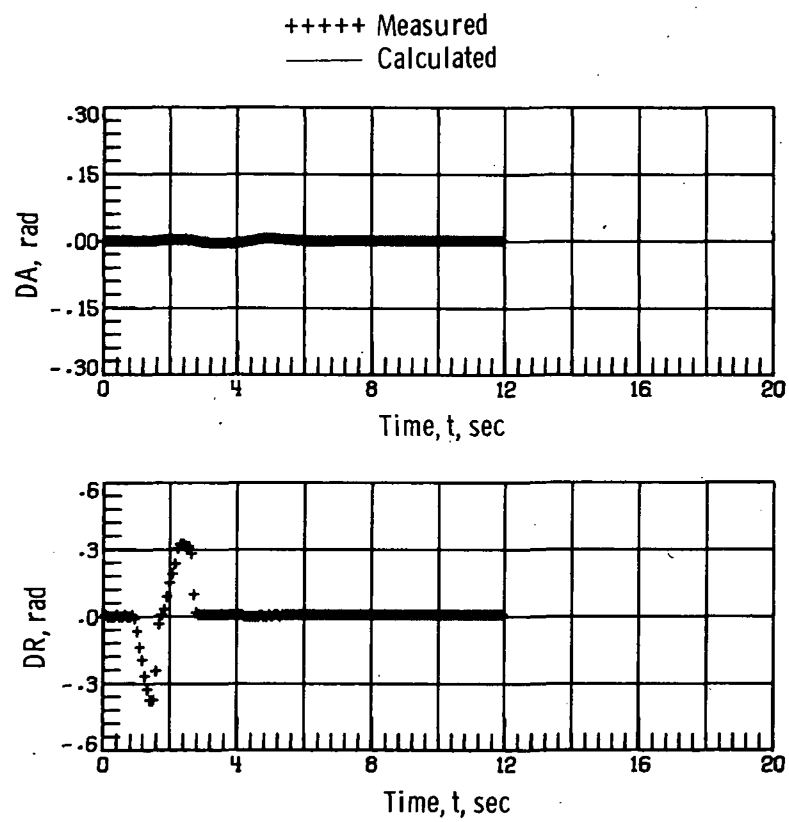

Figure 8.- Concluded.

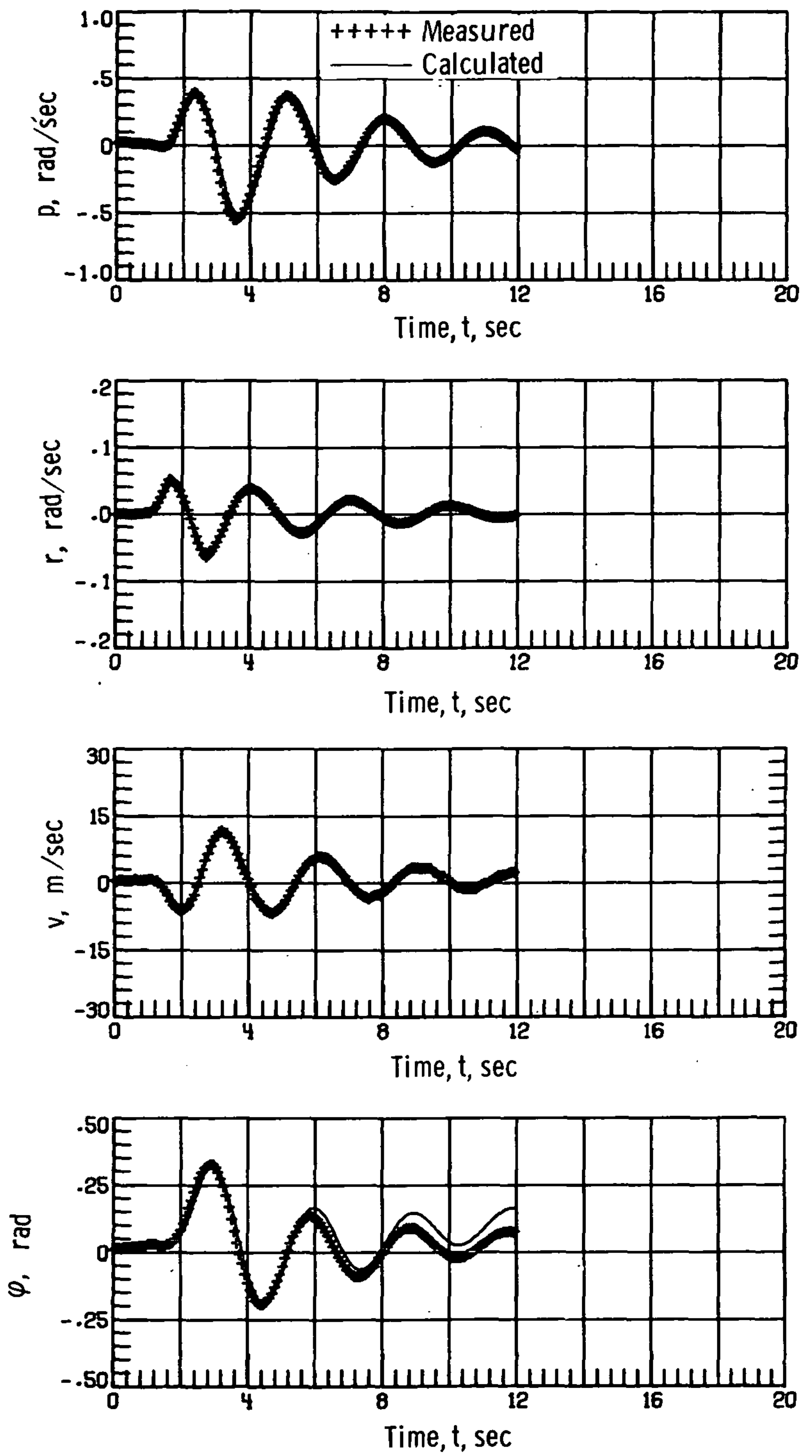

(a) $C_{l_r} = 0.70$.

Figure 9.- Effect of C_{l_r} on the computed time histories based on rudder input at $M = 0.90$.

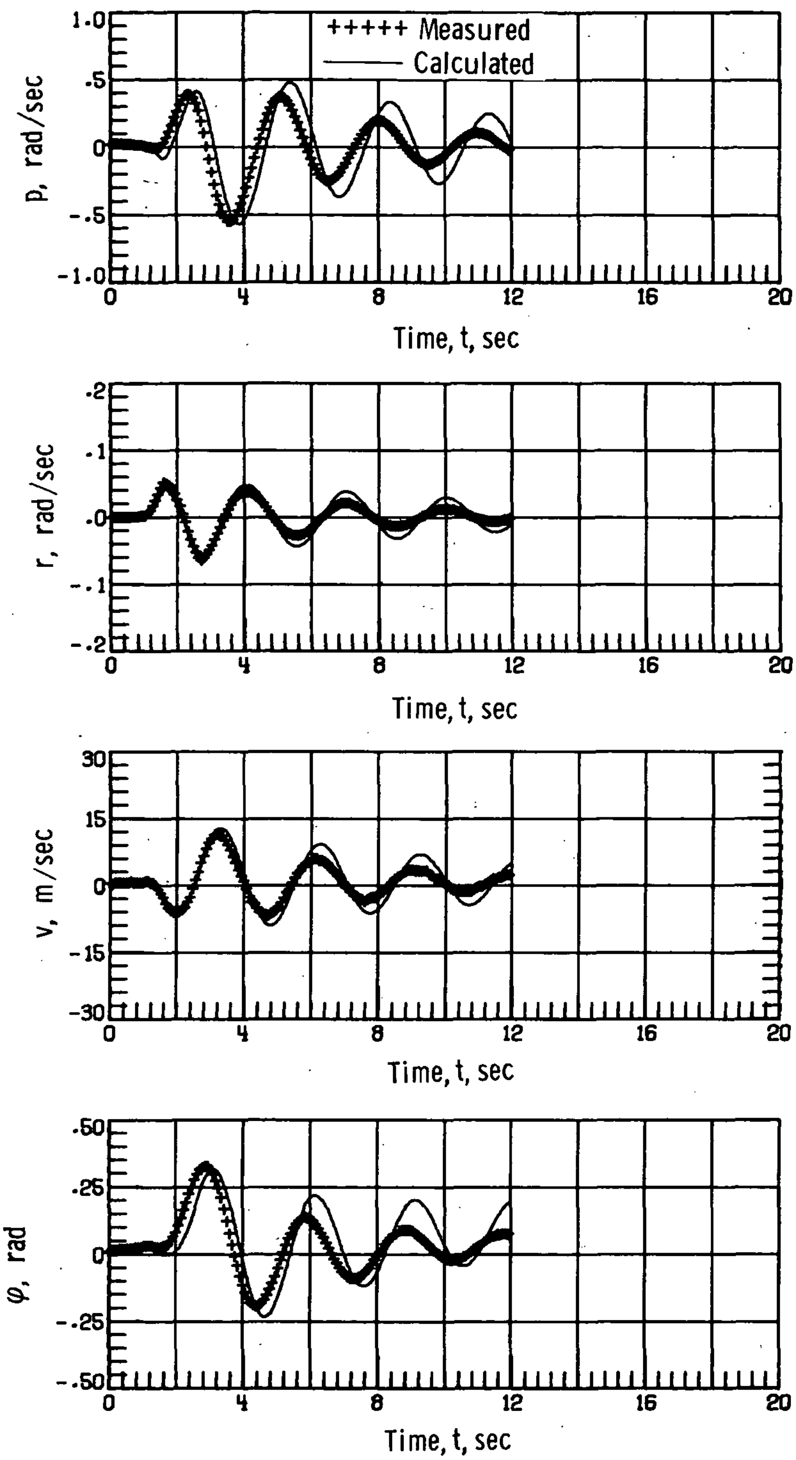

(b) $C_{l_r} = -0.70$.

Figure 9.- Continued.

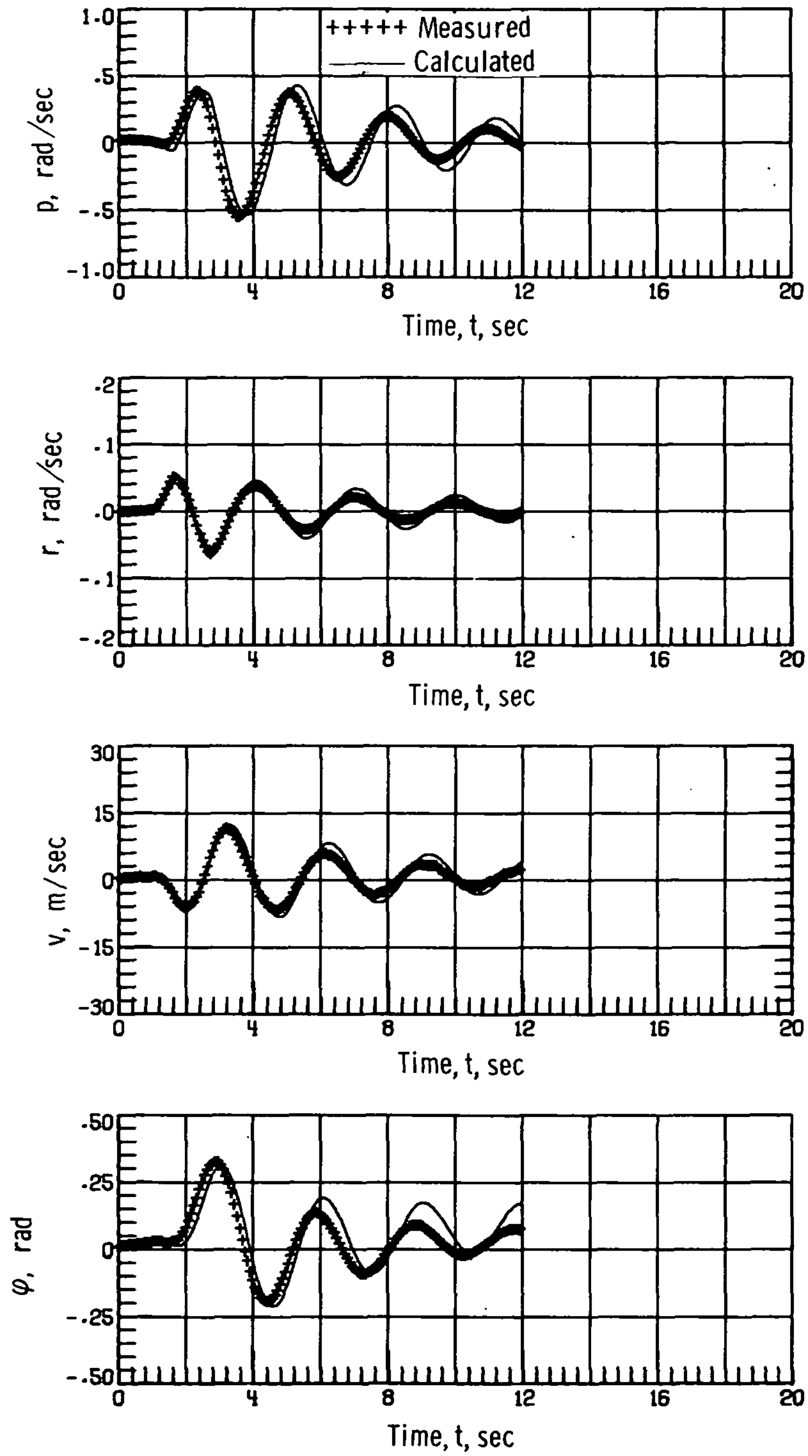

(c) $C_{l_r} = -1.57$.

Figure 9.- Concluded.

NATIONAL AERONAUTICS AND SPACE ADMINISTRATION
WASHINGTON, D.C. 20546

OFFICIAL BUSINESS
PENALTY FOR PRIVATE USE $300

SPECIAL FOURTH-CLASS RATE
BOOK

POSTAGE AND FEES PAID
NATIONAL AERONAUTICS AND
SPACE ADMINISTRATION
451

U.S.MAIL

POSTMASTER : If Undeliverable (Section 158 Postal Manual) Do Not Return

"The aeronautical and space activities of the United States shall be conducted so as to contribute . . . to the expansion of human knowledge of phenomena in the atmosphere and space. The Administration shall provide for the widest practicable and appropriate dissemination of information concerning its activities and the results thereof."

—NATIONAL AERONAUTICS AND SPACE ACT OF 1958

NASA SCIENTIFIC AND TECHNICAL PUBLICATIONS

TECHNICAL REPORTS: Scientific and technical information considered important, complete, and a lasting contribution to existing knowledge.

TECHNICAL NOTES: Information less broad in scope but nevertheless of importance as a contribution to existing knowledge.

TECHNICAL MEMORANDUMS: Information receiving limited distribution because of preliminary data, security classification, or other reasons. Also includes conference proceedings with either limited or unlimited distribution.

CONTRACTOR REPORTS: Scientific and technical information generated under a NASA contract or grant and considered an important contribution to existing knowledge.

TECHNICAL TRANSLATIONS: Information published in a foreign language considered to merit NASA distribution in English.

SPECIAL PUBLICATIONS: Information derived from or of value to NASA activities. Publications include final reports of major projects, monographs, data compilations, handbooks, sourcebooks, and special bibliographies.

TECHNOLOGY UTILIZATION PUBLICATIONS: Information on technology used by NASA that may be of particular interest in commercial and other non-aerospace applications. Publications include Tech Briefs, Technology Utilization Reports and Technology Surveys.

Details on the availability of these publications may be obtained from:

SCIENTIFIC AND TECHNICAL INFORMATION OFFICE

NATIONAL AERONAUTICS AND SPACE ADMINISTRATION

Washington, D.C. 20546